The relative importance of Antarctic sea-ice loss within the response to greenhouse warming

Stephanie Hay,[a] Paul J. Kushner,[b]

[a] *University of Exeter, Exeter, UK*

[b] *University of Toronto, Toronto, ON, Canada*

Corresponding author: Stephanie Hay, s.e.hay@exeter.ac.uk

ABSTRACT: The response to Antarctic sea-ice loss within a coupled modelling framework is examined in comparison to the response to Arctic sea-ice loss and within the context of general greenhouse warming. Sea-ice loss responses are found to be linear (particularly in response to Antarctic or global sea-ice loss) with respect to the degree of imposed perturbation and additive when perturbations are applied in hemispheres separately and concurrently. Globally, and in the tropical Pacific in particular, Antarctic sea-ice loss plays a relatively larger role than Arctic sea-ice loss in both the atmosphere and the ocean, within the parameters of our experiments. The pattern of response to Antarctic sea-ice loss is found to more closely resemble that of greenhouse warming, again particularly in the tropics. An extension to multi-parameter pattern scaling is developed to include a scaling factor for Antarctic change in addition to those for tropical warming and Arctic sea-ice loss. The decomposition is applied to the modelled response to Antarctic sea-ice loss to break it down into component partial responses that scale with Antarctic, tropical, and Arctic changes. This helps to reveal the aspects of the response that are directly related to Antarctic change, and those that are modified via the induced changes in the tropics and Arctic. With this, we hope to gain a deeper understanding of the role of each of these changes for the development of physical mechanisms of the response.

1. Introduction

While there exist many studies on the role Arctic sea-ice loss plays in the atmospheric response to greenhouse warming (Deser et al. 2015; McCusker et al. 2017; Blackport and Kushner 2017; Oudar et al. 2017; Sun et al. 2018), comparatively little work has been done on the role of Antarctic sea-ice loss (England et al. 2020b,a; Ayres and Screen 2019; Ayres et al. 2022). This disparity may be related to deficiencies of climate models in simulating Antarctic sea ice. For example, the Coupled Model Intercomparison Project Phase 5 (CMIP5; Kay et al. (2015)) models simulate a decrease in Antarctic sea ice over the historical period and project it to continue in to the 21st century, much as they do in the Northern Hemisphere (Turner et al. 2013). In reality, we have observed a small increase over the last 40 years (Turner et al. 2013; Zunz et al. 2013). The cause of this discrepancy between models and observations has been the focus of many studies, with a particular focus on how large internal variability of the Antarctic can in fact align the observed increase in area with model simulations (Swart and Fyfe 2013; Gagné et al. 2015; Singh et al. 2019). The latest generation of climate models participating in the Coupled Model Intercomparison Project Phase 6 (CMIP6; Eyring et al. (2016)) have reduced the spread of the simulated seasonal cycle of Antarctic sea ice, however there continues to be less confidence in projections of Southern Hemisphere sea ice than its northern counterpart due to deficiencies in simulating the mean state (Roach et al. 2020). Nonetheless, the role of Antarctic sea-ice within the response to greenhouse warming remains an important question, and we seek to understand the climate response to a loss of Antarctic sea ice so that, at the very least, we may be able to understand climate model biases in terms of the response to Antarctic sea-ice biases.

We find a small scope of modelling studies devoted to isolating the atmospheric response to Antarctic sea-ice loss in atmosphere-only configurations (Kidston et al. 2011; Bader et al. 2013; England et al. 2018) and in coupled model configurations (Smith et al. 2017; England et al. 2020b,a; Ayres et al. 2022). Within the former, Kidston et al. (2011) find increasing the extent of the sea ice leads to a significant poleward shift in the mid-latitude jet in the cold season only, while decreasing the extent led to no significant response. The authors conclude that future Antarctic sea-ice loss is unlikely to have an impact on the mid-latitude circulation. In contrast, Bader et al. (2013) found that the mean response in the cold season resembled the negative phase of the Southern Annular Mode (SAM), with an equatorward shift of the mid-latitude jet. England et al. (2018) also find a small but significant equatorward shift of the jet. Within the latter, the England et al. studies focus mainly on the response in the tropics, where the authors find a strong response to both Arctic and Antarctic sea-ice loss of approximately equal magnitude, of which the Antarctic response is crucial in generating additional Arctic sea-ice loss and warming via a teleconnection driven by the tropicals response. The results of Ayres et al. (2022) are in broad agreement with those of England et al., but they also include an examination of the oceanic response, which supports the ideas of England et al. (2020a).

Smith et al. (2017) uses a coupled model setup that constrains ocean temperature and salinity below 200m, therefore making it somewhat more akin to a slab ocean rather than a full dynamical ocean, and additionally simulates the response to the small positive trend that has been observed rather than the larger projected changes of the end of the century. Nevertheless, they do find a poleward shift of the mid-latitude jet in response to increased Antarctic sea-ice area. Finally, a study by Ayres and Screen (2019) uses a combination of coupled and atmosphere-only experiments from the CMIP5 archives to determine the response to sea-ice loss as a residual, using the indirect method of Zappa et al. (2018). Ayres and Screen (2019) find that Antarctic sea-ice loss acts to oppose the positive SAM response to increased CO_2 mainly through a weakening of the eddy-driven jet rather than an equatorward shift.

Typically, modelling studies that have focused on the Northern Hemisphere coupled climate response to sea-ice loss have assumed that the impact of Southern Hemisphere sea-ice melt on the Northern Hemisphere is negligible (Blackport and Kushner 2016, 2017; Hay et al. 2018; Screen and Blackport 2019; Sun et al. 2020; Hay et al. 2022). The work of England et al. (2020a) showed that Antarctic sea-ice melt generates a response in the tropical Pacific Ocean, which may then itself generate a response in the Northern Hemisphere extratropics. The global nature of the response to Antarctic forcing has also previously been found in a study by Bronselaer et al. (2018). The authors of that study showed how freshwater input near the Antarctic continent, intended to approximate expected melt from the Antarctic ice sheet, can increase the Southern Hemisphere sea-ice area, which results in delayed warming relative to RCP8.5 forcing, and a drying of the Southern Hemisphere.

As additional evidence for a potentially important role remote responses to Antarctic change, there also exists a body of literature on how changes in the Southern Hemisphere polar and extratropical regions, not necessarily related to sea ice, can generate a response in the tropics. For example, Kang et al. (2008) highlighted how extratropical thermal anomalies can shift the ITCZ location, and Kang et al. (2011) showed that Southern Hemisphere polar ozone depletion can cause shifts in the westerly jet that alter subtropical precipitation.

This study seeks to examine the relative role of Antarctic and Arctic sea-ice loss within the larger greenhouse warming response. We use of a suite of simulations where the albedo of sea ice is perturbed in each hemisphere separately and in both hemispheres concurrently under two different albedo parameter settings. The two different parameter settings allow us to assess the linearity of the response, while the separate and concurrent settings allow us to assess the additivity of the responses. We then make use of pattern-scaling methods to used to decompose the responses as in previous work (Blackport and Kushner 2017; Hay et al. 2018; Feldl et al. 2020; Hay et al. 2022), but with the inclusion of a parameter related to Antarctic change. With this, instead of decomposing the response to greenhouse warming as has been done previously, we explore a new application of pattern scaling by decomposing the response to Antarctic sea-ice loss to understand aspects of its global nature.

This paper is organized as follows: Section 2 presents the suite of simulations used herein and a brief derivation of an improved three-parameter pattern-scaling method. Section 3 is made of of two distinct parts: in the first, we discuss the linearity and additivity of the response to sea-ice loss from each hemisphere and use a spatial correlation analysis to reveal the relative importance of Antarctic sea-ice loss compared to the Arctic within the response to global warming. Next, we apply three-parameter pattern-scaling to our suite of simulations and explore using other, more physically motived, scaling parameters. With this, we show how various parts of the response to Antarctic sea-ice loss are re-inforced or masked by the tropical and Arctic change it induces. Section 4 presents a summary of the results and discussion within the existing literature, and finally Section 5 presents a brief summary of the presented results and conclusions.

2. Methods

a. Simulations

To determine the relative contributions of Arctic and Antarctic sea-ice loss within the response to greenhouse warming, we perform eight simulations with the Coupled Earth System Model,

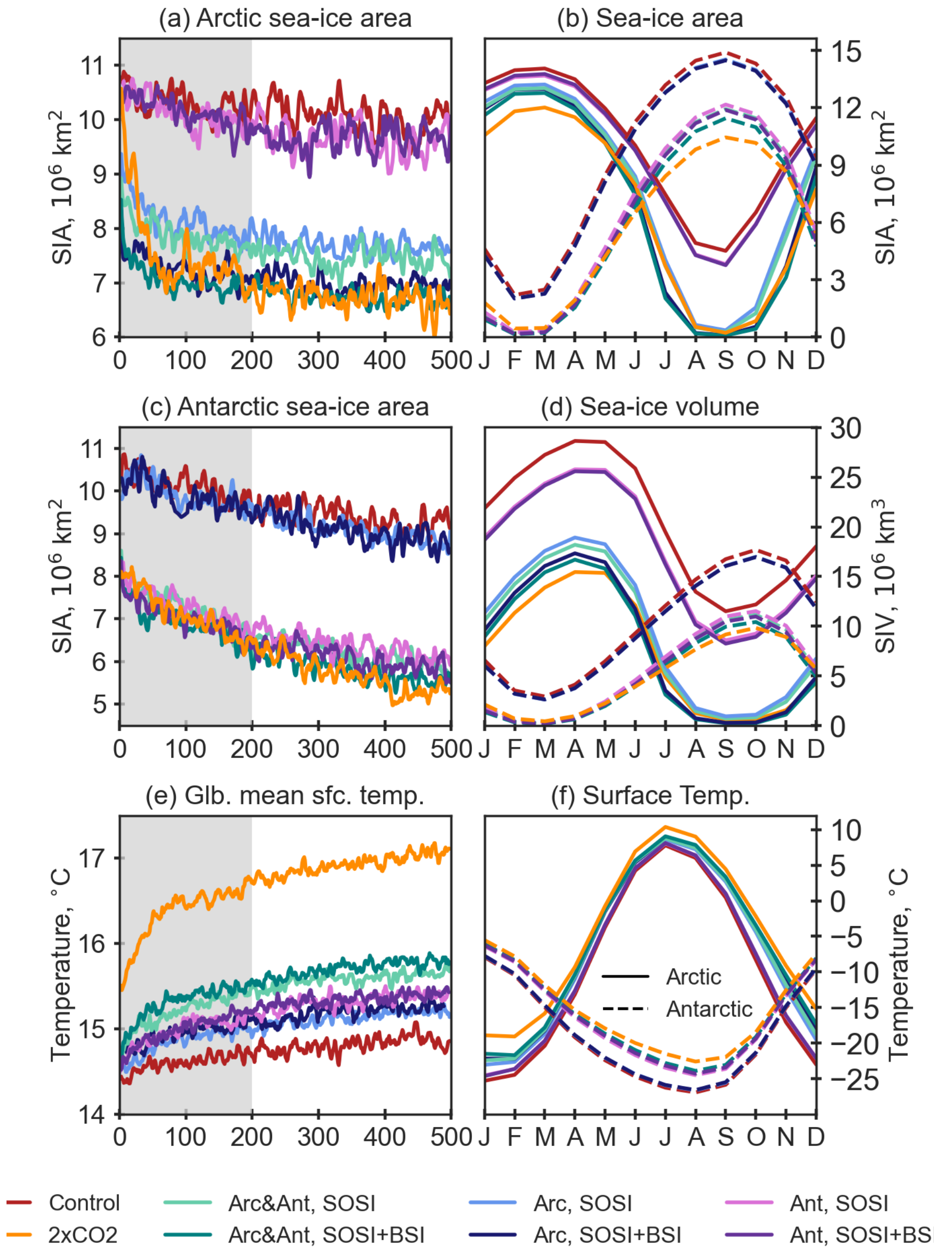

FIG. 1. Timeseries of five-year-running mean and seasonal cycles of sea-ice and temperature fields are shown. In (a) and (c) are the time series of Arctic and Antarctic sea-ice area, respectively, and in (e) is the time series of global mean surface temperature, where the red represents "control", the orange "2xCO_2", light teal "Arc & Ant, SOSI", dark teal "Arc & Ant, SOSI+BSI", light blue "Arc, SOSI", dark blue "Ant, SOSI", light purple "Ant, SOSI", and dark purple "Ant, SOSI+BSI". In (b), (d), and (f) are seasonal cycles of sea-ice area, sea-ice volume, and surface temperature, over the Arctic region in solid lines, and over the Antarctic in dashed lines.

TABLE 1. The simulation nomenclature used in this paper, with the radiative forcing, perturbed values applied to Arctic and Antarctic snow on sea ice and sea ice albedos,

Simulation name	Radiative forcing	Arctic albedo perturbation	Antarctic albedo perturbation
Control	Year 2000	None	None
$2\times CO_2$	$2\times$PI CO_2	None	None
Arc& Ant, SOSI	Year 2000	*R_snw*=-6.0	*R_snw*=-6.0
Arc& Ant, SOSI+BSI	Year 2000	*R_snw*=-6.0, *R_ice*=-6.0	*R_snw*=-6.0, *R_ice*=-6.0
Arc, SOSI	Year 2000	*R_snw*=-6.0	None
Arc, SOSI+BSI	Year 2000	*R_snw*=-6.0, *R_ice*=-6.0	None
Ant, SOSI	Year 2000	None	*R_snw*=-6.0
Ant, SOSI+BSI	Year 2000	None	*R_snw*-6.0, *R_ice*=-6.0

Version 1 (CESM1) using the CESM Large Ensemble (LENS) version used by Kay et al. (2015) and a sea-ice loss protocol that acts on the albedo of bare sea ice and snow on sea ice, similar to that of Blackport and Kushner (2017). CESM1 is a fully-coupled earth system model with nominal resolution of 1° in both the atmosphere and the ocean, for more details see Kay et al. (2015) and references therein.

Outlined in Table 1, these simulations are each branched at Year 2000 of the CESM LENS member 1 and integrated for 500 years to quasi-equilibrium, of which we retain the last 300 years for analysis. First, we have a "control" simulation with perennial year 2000 radiative forcing, and a "2xCO_2" simulation where CO_2 is instantaneously increased to 560 ppm, twice the preindustrial concentration. The difference between these two simulations we take to be the response to greenhouse warming, which is understood to be dominated by CO_2 forcing. Next, we perform three experiments where we perturb the albedo of the snow on the sea ice (SOSI) in each hemisphere separately ("Arc, SOSI" and "Ant, SOSI"), and in both concurrently ("Arc & Ant, SOSI") to rapidly melt sea ice. Specifically, the variable *R_snw* within the sea ice shortwave module is set to -6.0 in order to increase the grain size of snow, and thus decrease its albedo (Briegleb and Light 2007). Finally, we repeat these experiments but we additionally perturb the albedo of the bare sea ice (BSI) as well to get the "Arc, SOSI+BSI", "Ant, SOSI+BSI", and "Arc & Ant, SOSI+BSI". This perturbation is accomplished by setting both $R\_snw = -6.0$ and $R\_ice = -6.0$, with the latter having the effect of decreasing the albedo of bare ice by six standard deviations. In the

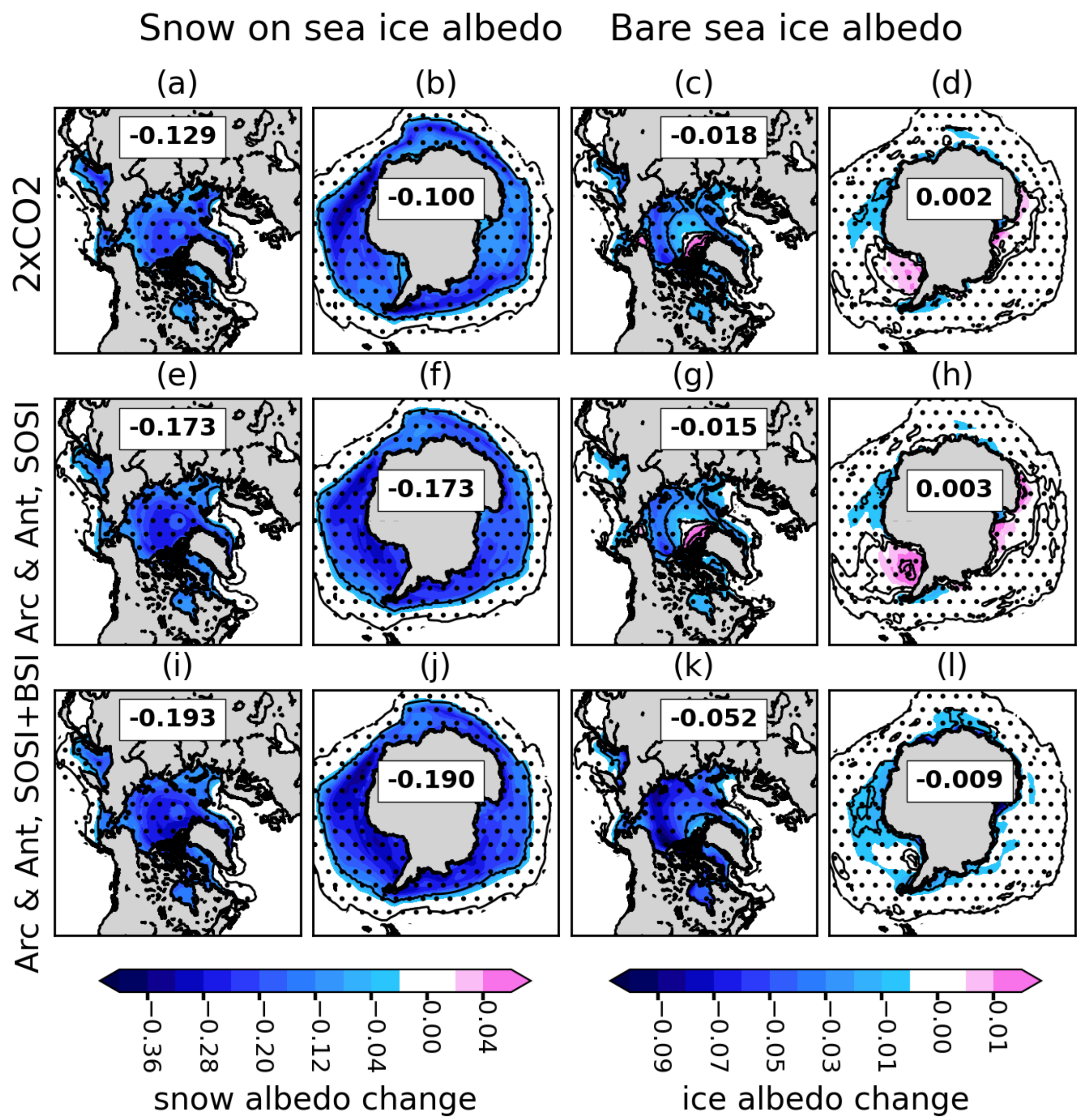

FIG. 2. Responses in sea ice albedos are shown. In (a) – (d) are the response of albedo of snow on sea ice in "2xCO_2" the Northern Hemisphere, in the Southern Hemisphere, of the bare sea ice albedo in the Northern Hemisphere, and in the Southern Hemisphere, respectively. (e) – (h) and (j) – (l) are as in (a) – (d) but for the response in "Arc & Ant, SOSI" and "Arc & Ant, SOSI+BSI", respectively. Stippling indicates where the albedo response is significant at the 95% confidence level.

"SOSI+BSI" simulations, approximately 3×10^6 km^2 of sea ice is lost in the annual mean in the perturbed hemisphere, which closely matches that lost under greenhouse warming (Fig. 1). The difference between each of these six simulations and "control" gives us the response to Arctic sea-ice loss, to Antarctic sea-ice loss, and to Arctic and Antarctic sea-ice loss, under two levels of sea-ice loss forcing. In addition to the additivity of the response to sea-ice loss we obtain with the first set of albedo perturbation experiments, the second set of allow us to assess the the linearity to different strengths of sea-ice forcing.

Examining the first few years in Fig. 1(a) and (c) we see that both albedo parameter settings result in rapid (within a few years) sea-ice loss in each hemisphere, while sea-ice loss in the CO_2 doubling scenario adjusts somewhat slower (on the order of 50 years) in the Arctic but just as rapidly as it does under albedo forcing in the Antarctic. After 100 years of simulation, the "SOSI+BSI" experiments and the CO_2 doubling experiment have approximately the same amount of sea-ice loss. We note that the Antarctic sea-ice area continues to drift throughout much of our simulations, appearing to be approaching quasi-equilibrium only after 400 or so years, whereas the Arctic is quasi-equilibrated within 100 years. This drift is also apparent in the global mean surface temperature (Fig. 1(e)). We do not expect it to be the result of the albedo perturbation because both the control simulation and "2xCO_2" simulation undergo ongoing adjustment as well. Instead, we suspect that it is the result of Southern Ocean upwelling, when deep water formed in the Northern Hemisphere upwells in the Southern Ocean at long timescales (Talley 2013). A similar slow drift was also found in the experiments of Ayres et al. (2022).

Approximately 1/4 (0.5°C) of global mean surface warming in 2×CO_2 (2°C) is found in the "Arc & Ant, SOSI+BSI" albedo forcing experiment (Fig. 1(e)). When albedo forcing is constrained to the Antarctic only, there is somewhat more global warming than when the forcing is constrained to the Arctic only. In the tropics (not shown), less than 1/10 of the sea-surface warming resulting from the CO_2 doubling experiment occurs when albedo forcing in applied in the Arctic only, while 1/5 of the SST warming occurs when albedo forcing applied in the Antarctic only, while roughly 1/4 of the total warming occurs when albedo forcing is applied globally.

The seasonal cycle of sea-ice area (Fig. 1(b)) reveals that while our experiments are effective at reproducing the annual mean sea-ice loss under a doubling of CO_2, they overestimate sea-ice loss in the summertime and underestimate it in the wintertime in both hemispheres. The result is an

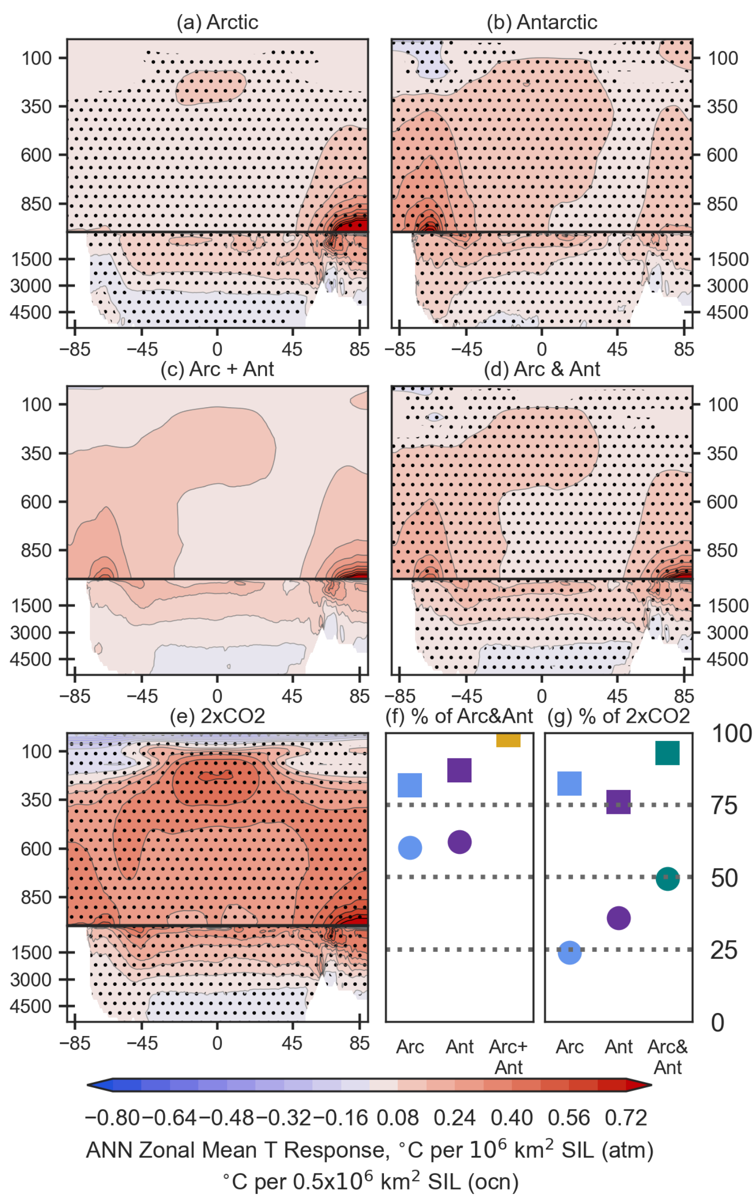

FIG. 3. The response in zonal mean atmospheric and oceanic temperature are shown, scaled by the sea-ice area lost as in Table 1. In (a) is the response in the "Arc, SOSI+BSI" simulation, in (b) for "Ant, SOSI+BSI", in (c) is the sum of (a) and (b), in (d) for the "Arc & Ant, SOSI+BSI", in (e) for the "2×CO_2". Stippling in (a), (b), (d), and (e) indicates where the response is statistically significant at the 95% confidence level. (f) gives the spatial variance (i.e., the square of the spatial correlation) of "Arc&Ant, SOSI+BSI" explained by "Arc" in blue, "Ant" in purple, and their sum in gold. The circles represent the variances for the atmosphere and the squares represent the variances for the ocean. In (g) as in (f) but for the variance of "2×CO_2" explained by "Arc", "Ant", again in blue in purple, and "Arc&Ant" in teal.

amplified seasonal cycle of sea-ice area compared to greenhouse forcing. This deficiency in using a shortwave forcing method, in that it is most effective when there is incoming shortwave, thus missing the all-important winter ice loss, has been pointed out in previous work (Deser et al. 2015; Sun et al. 2020). We note here that the more equatorward position of Antarctic sea ice relative to Arctic sea ice means that this method can be more effective in the Southern Hemisphere. Indeed, July-August-September sea-ice loss in the Southern Hemisphere in "Arc & Ant, SOSI+BSI" is underestimated by 19% relative to "2xCO_2", and December-January-February sea ice by 30% in the Northern Hemisphere.

Albedo forcing is effective at reducing the volume of sea ice in both hemispheres (Fig. 1(d)), indicating that the sea ice that forms each winter is very thin. The seasonal cycle also reveals that albedo forcing in the Antarctic is more effective at making changes in the Arctic than vice-versa, with more separation between the solid red and purple lines than between the dashed red and blue lines in Fig. 1(b) and (d). The annual mean sea-ice area loss in the Northern Hemisphere due to Antarctic albedo forcing shown is 50% greater than the annual mean sea-ice area loss in the Southern Hemisphere due to Arctic albedo forcing.

The seasonal cycle of surface temperature averaged poleward of 60° in each hemisphere is shown in Fig. 1(f). Despite the overestimation of sea-ice loss compared to CO_2 doubling, the surface warming is underestimated in summertime. The cause of this difference may be related to other changes in the polar regions that occur only under CO_2 forcing and not under albedo forcing, such as changes in heat transport or clouds. The $2\times CO_2$ and "SOSI+BSI" albedo forcing curves match closely in Spring and nearly in Autumn in both hemispheres. There is little difference in the amount of warming between the "SOSI" and "SOSI+BSI" albedo forcing scenarios in wintertime and slightly more separation in summer, in each hemisphere.

b. Three-parameter pattern scaling

Coupled ocean-atmosphere models permit a full dynamical adjustment of the climate through the inclusion of thermodynamic and dynamics feedbacks between the ocean and atmosphere (Deser et al. 2015, 2016; Tomas et al. 2016), which extends the global reach of the sea-ice response. But this introduces some ambiguity in the mid-latitude response to sea-ice loss because the lower-latitude warming that occurs in a fully coupled experiment can in turn impact the mid-latitude

TABLE 2. The amount of tropical (20°S to 20°N) sea surface warming, Arctic sea-ice loss, Antarctic sea-ice loss, as well as the change in the upper tropospheric (300-700 hPa) tropical lapse rate, the lower tropospheric (1000-900 hPa) Arctic (> 65°N) lapse rate, and the lower tropospheric (975-800 hPa) Antarctic (< 65°S) lapse rate in the annual mean, relative to "control" for each of the simulations in Table 1

Response	δT^{trop} (°C)	δI^{Arc} (10^6 km^2)	δI^{Ant} (10^6 km^2)	$\delta\Gamma^{trop}_{upper}$ (K km^{-1})	$\delta\Gamma^{Arc}_{lower}$ (K km^{-1})	$\delta\Gamma^{Ant}_{lower}$ (K km^{-1})
2×CO_2	1.06	-3.22	-3.42	0.25	-2.11	-0.63
Arc & Ant, SOSI	0.26	-2.58	-3.12	0.06	-2.26	-0.80
Arc & Ant, SOSI+BSI	0.29	-3.32	-3.44	0.07	-2.80	-0.89
Arc, SOSI	0.07	-2.33	-0.24	0.02	-2.17	-0.05
Arc, SOSI+BSI	0.09	-3.11	-0.26	0.02	-2.73	-0.04
Ant, SOSI	0.20	-0.36	-2.95	0.04	-0.21	-0.78
Ant, SOSI+BSI	0.21	-0.39	-3.23	0.05	-0.23	-0.85

response. This "back-effect" of the low-latitude response on the extratropics can be accounted for with *multi-parameter pattern scaling* (Blackport and Kushner 2017; Hay et al. 2018; Feldl et al. 2020; Hay et al. 2022).

Additivity and separability of the atmospheric response to sea-ice loss from the rest of the greenhouse warming response has been demonstrated in McCusker et al. (2017), and two-parameter parameter scaling, first introduced by Blackport and Kushner (2017), has been used in the studies of Hay et al. (2018, 2022); Feldl et al. (2020) to facilitate an inter-model comparison of non-coordinated sea-ice loss experiments, and to understand high-latitude climate feedbacks. The idea is as follows: assuming that a field-like variable Z, which could represent any atmospheric or oceanic field, depends parameterically on internal variables X_i (e.g. mean surface temperature, sea-ice extent) we can use pattern scaling approaches to estimate the *sensitivity* of Z to each internal variable, or *scaling parameter* (while the other parameters are held fixed). Symbolically, this sensitivity is written $\frac{\partial Z}{\partial X_i}\Big|_{X_j \neq X_i}$, If a model simulation generates a forced response δZ_m for a particular type of forcing, the response can be written as the sum of *partial responses*,

$$\delta Z_m = \sum_i \frac{\partial Z}{\partial X_i}\bigg|_{X_j \neq X_i} \delta X_{i,m}, \qquad (1)$$

Unlike in previous work on this topic that considered the two-parameter problem (using Arctic sea-ice area and low-latitude sea surface temperature as the scaling parameters), the independent

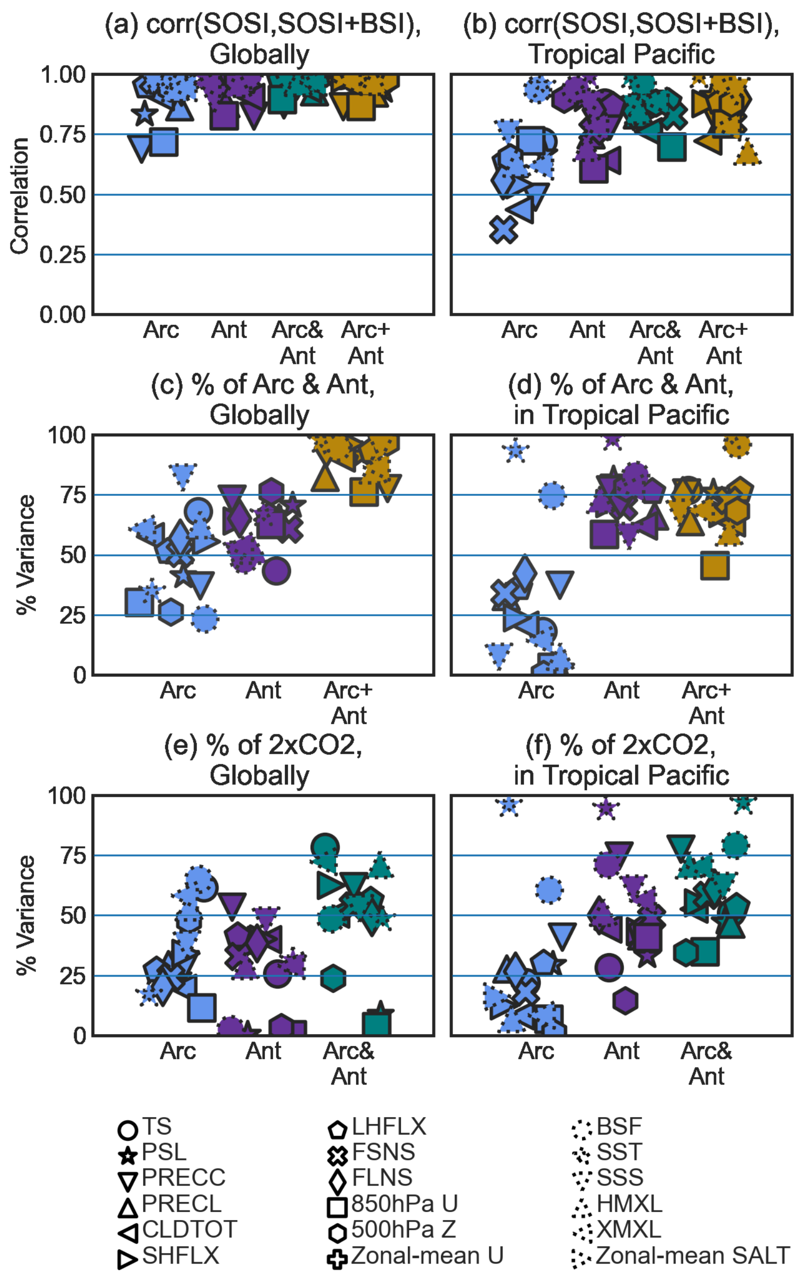

FIG. 4. The spatial correlation between the equivalent "SOS" and "SOSI+BSI" to demonstrate linearity of responses (a) globally and (b) over the tropical Pacific Ocean. The amount of spatial variance in the "Arc & Ant, SOSI+BSI" ((d) for the entire globe, (d) for the tropical Pacific region) and "2×CO_2" responses ((e), (f)) that can explained by the "Arc, SOSI+BSI" in blue, "Ant, SOSI+BSI" in purple, "Arc&Ant, SOSI+BSI" in teal, and "Arc + Ant, SOSI+BSI" in gold. Solid edges on the markers indicate atmospheric variables while dashed edges indicate oceanic variables.

and distinct response patterns to greenhouse forcing, Arctic sea-ice loss, and Antarctic sea-ice loss presented below and as shown in England et al. (2020b,a), obtained by separately controlling sea-ice area from radiative forcing, motivate the inclusion of a third scaling parameter, one related to Antarctic forcing. More generally, we use scaling parameters to represent Antarctic forcing, δAA, Arctic forcing, δA, and tropical forcing, δT and represent the forced response in some variable, δZ_m, as the sum of partial response patterns,

$$\delta Z_m = \left.\frac{\partial Z}{\partial A}\right|_{T,AA} \delta A_m + \left.\frac{\partial Z}{\partial AA}\right|_{A,T} \delta AA_m + \left.\frac{\partial Z}{\partial T}\right|_{A,AA} \delta T_m \tag{2}$$

Pattern scaling is based on an assumption of additivity of internal and external climate forcings. It is generally implicitly assumed that climate responses to external forcings (e.g., CO_2, anthropogenic aerosols, ozone, volcanic eruptions) can be linearly added to obtain the total climate response to the sum of the forcings (Stott et al. 2010). While some variables like temperature are generally additive, it breaks down in other fields such as precipitation under some forcing scenarios (Shiogama et al. 2013; Marvel et al. 2015). The additivity of the climate response to internal forcing agents, such as sea-ice area, SSTs, and lapse rates, has some evidence in support of it (McCusker et al. 2017; Oudar et al. 2017; Hay et al. 2022). We can expect to obtain the best results from this method as long as we remain within a linear regime, which we attempt to assess for these experiments below, and have sufficient sampling, given to us by multiple multi-centennial simulations.

3. Results

a. Albedo response

The annual mean response of the albedo of snow on sea ice and bare ice are shown in Fig. 2 for "2xCO_2", "Arc & Ant, SOSI", and "Arc & Ant, SOSI+BSI". We do not include the single hemisphere simulations because their responses are very similar to the equivalent "Arc & Ant" response, albeit with slightly reduced magnitude. We note the high degree of similarity of the albedo response of snow on sea ice in our perturbed simulations to that obtained via a CO_2 doubling (Fig. 2(a) and (b) compared to (e) and (f) and (j) and (i)). The decrease in the albedo of snow on sea ice under CO_2 doubling results from the warmer, wetter snow (Perovich et al. 2002) as

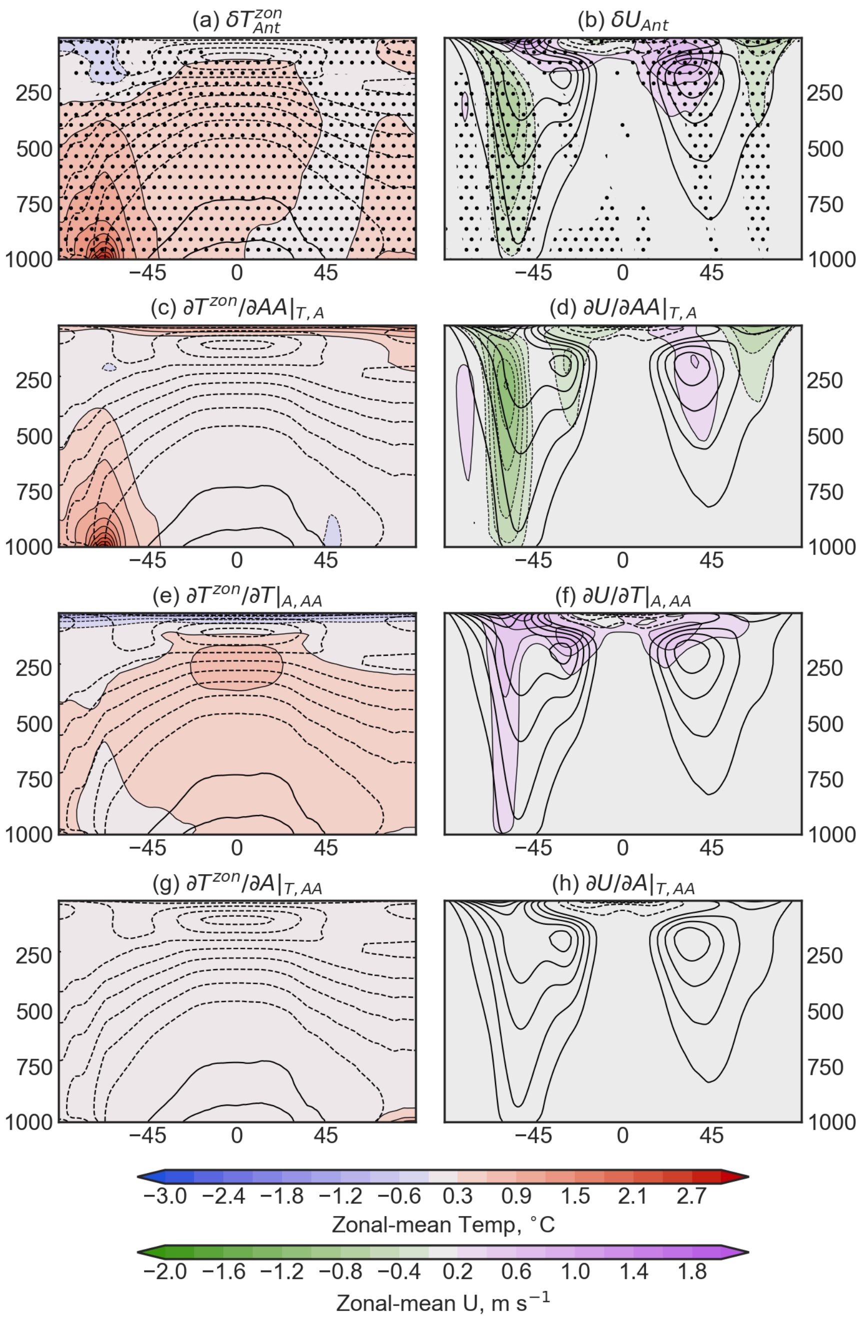

FIG. 5. In filled contours are the zonal-mean temperature (a) and zonal-mean zonal wind (b) responses to Antarctic sea-ice loss decomposed in to three partial responses: (c) and (d) are the partial responses to Antarctic sea-ice loss, (e) and (f) are the partial responses to tropical warming, and (g) and (h) are the partial responses to Arctic sea-ice loss. The solid and dashed black contours show the zonal-mean temperature and zonal-mean zonal wind in "control", where solid indicate positive values and dashed indicate negative values. Stippling in (a) and (b) indicate where the response to Antarctic sea-ice loss is statistically significant at the 95% confidence level.

temperatures increase from radiative forcing. The magnitude of change, averaged over all grid boxes with sea-ice present, is 1.3-1.7 times larger for the "SOSI" response, and 1.5-1.9 times larger for the "SOSI+BSI" response. Perturbing the albedo of the snow on sea ice only results in small changes to the albedo of bare ice that approximately match those of "2×CO_2" (Fig. 2(c) and (d) compared to (g) and (h). On the other hand, when we perturb the bare ice, we find a different response pattern in its albedo (Fig. 2(k) and (l)), with none of the regions of increasing albedo found otherwise.

It is clear that perturbing *R_snw* is much more effective at changing the albedo of snow on sea ice than perturbing *R_ice* is for changing the albedo of bare ice, particularly in the Southern Hemisphere. The average albedo of snow on sea-ice in the control simulation is 0.43 and 0.49, averaged across all grid-boxes containing sea ice, in the Northern and Southern Hemispheres, respectively. These are reduced to 0.30, 0.26, 0.24, and 0.39, 0.32, 0.30, in "2xCO_2", "Arc & Ant, SOSI", and "Arc & Ant, SOSI+BSI", for the Northern and Southern Hemispheres, respectively. On the other hand, the average albedo of bare ice is only 0.06 and 0.01, respectively, in the annual mean. These values are reduced to 0.04, 0.04, 0.01 in the Northern Hemisphere and less than 0.01 for all simulations in the Southern Hemisphere. These apparent very small values of bare ice albedo result from the extensive snow cover on the ice, particularly in the Antarctic (Massom et al. 2001), which leave little areal coverage of bare ice and reduce the impact, on a hemispheric scale, of perturbing bare ice albedo.

Perturbing the value of *R_ice* on top of changing the albedo of snow on sea ice is not as effective at changing the albedo of the sea ice in the Southern Hemisphere due to the small area of bare ice in the model, while it can decrease by an additional 0.04, averaged over the Northern Hemisphere sea-ice area. In the Northern Hemisphere, the unperturbed response in albedo (Fig. 2(c)) results in an increase of the albedo of bare ice north of Greenland and a decrease elsewhere. Because these simulations result in an "ice-free" Arctic (the orange and light teal lines in Fig. 2(b)), the multi-year ice that typically makes up this region will be replaced by first-year ice with a higher albedo. Perturbing the albedo of bare ice counteracts this effect, save for a small region along the Greenland coast, and additionally decreases the albedo over the rest of the sea ice, achieving a hemispheric decrease. On the other hand, the response of the albedo of bare ice in the Southern Hemisphere is small both in the unperturbed simulations (Fig. 2(d)) and in the perturbed simulation (Fig. 2(l)).

As in the Northern Hemisphere, perturbing the albedo overcomes the otherwise positive response occurring in the Ross and Weddell Seas.

b. Linearity and Additivity

In Fig. 3, we show the zonal mean temperature response, scaled by the global sea-ice loss, of both the atmosphere and ocean for the "SOSI+BSI" simulations. The "SOSI" simulations generate similar responses with reduced magnitude. The familiar pattern of both polar lower tropospheric and tropical upper tropospheric warming is seen in the atmosphere, and we find it mirrored near the ocean surface. The similarity of panels (c) (which shows the sum of the responses to "Arc, SOSI+BSI" and "Ant, SOSI+BSI") and (d) (the response to "Arc & Ant, SOSI+BSI") indicate the additivity of sea-ice loss forcing from each hemisphere across the zonal mean thermal response. We quantify the degree of additivity (Fig. 3(f)) as the spatial variance in "Arc & Ant, SOSI+BSI" explained by "Arc, SOSI+BSI", "Ant, SOSI+BSI", and "Arc + Ant , SOSI+BSI", with the latter, in gold, being near 100% here. Somewhat more of the spatial variability comes from "Ant, SOSI+BSI" (57 and 80% for atmosphere and ocean, respectively), than for "Arc, SOSI+BSI" (55 and 75%). The similar but stronger pattern of response obtained from "2$\times$CO$_2$" can be seen in (e) and we quantify the similarity of the sea-ice loss response patterns by spatial variance explained in (g). It is lowest for the atmospheric response to "Arc, SOSI+BSI" at 25%, while nearly 100% of the spatial variance of the oceanic response is explained by "Arc & Ant, SOSI+BSI".

To more generally assess the linearity and additivity of the sea-ice loss responses, we first correlate the "SOSI" responses with their corresponding "SOSI+BSI" response for many atmospheric and oceanic fields and present them in Fig. 4(a). The correlation between responses to two different sea-ice forcings can be understood as an indirect test of linearity. The high correlations indicate a high degree of linearity exhibited by all variables in response to sea-ice loss, confirming previous research (Screen et al. 2018) and justifying the use of the linear decomposition of pattern scaling for understanding these responses. We note that the response to Arctic sea-ice loss appears to be slightly less linear than the response to Antarctic sea-ice loss. This result is particularly apparent in the tropical Pacific (b) where the response to Arctic sea-ice loss is fairly noisy in the "SOSI" experiment.

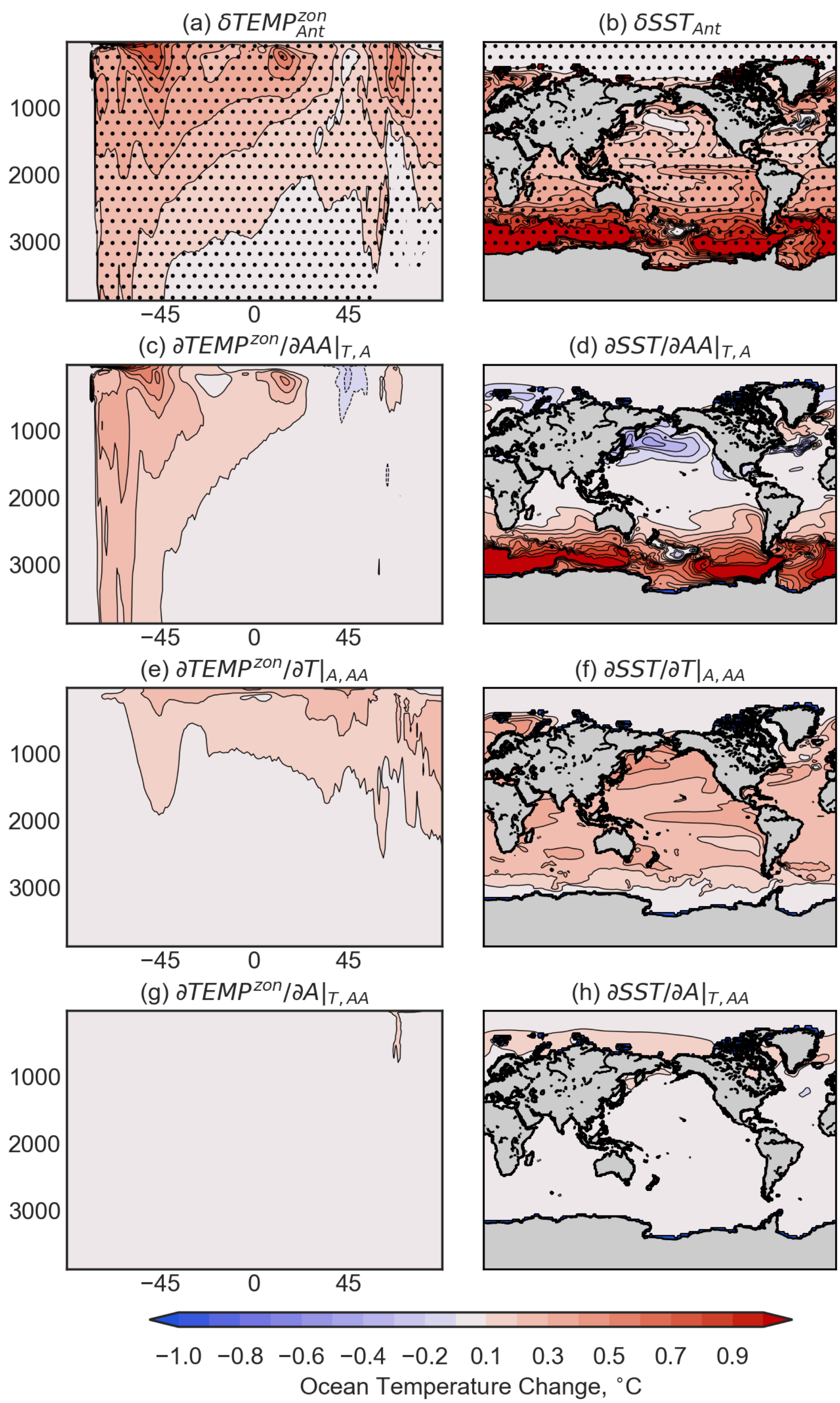

FIG. 6. As in Fig. 5 but for the zonal mean ocean temperature and sea surface temperature responses and partial responses.

Given the linearity of the responses, hereafter we will examine only the "SOSI+BSI" responses and for simplicity and reading ease, we will drop "SOSI+BSI" suffix to the experiment names as the "SOSI" results are very similar but the "SOSI+BSI" results have a better signal to noise ratio. A high degree of additivity is exhibited across all examined variables, in good agreement with the results of England et al. (2020b). The spatial variance of "Arc & Ant" (Fig. 4(c),(d)) explained by "Ant" is generally larger than that explained by "Arc", particularly so in the tropical Pacific region, where the response to Antarctic sea-ice loss is clearly dominant over the response to Arctic sea-ice loss. Additionally, we find the ocean is surprisingly linear and additive to sea-ice forcing, motivating the use of pattern-scaling on oceanic variables.

The response in "Arc & Ant" can explain, on average across different variables, about half the spatial variance in "2xCO_2" (Fig. 4(e), (f)). Each of "Arc" and "Ant" explain about the same amount, globally, but in the tropical Pacific it is clear that "Ant" more closely resembles the pattern from greenhouse warming.

c. Pattern-Scaling Results

Using an extension of pattern scaling to three parameters with the simulations at hand, we have $m \geq 3$ with $m = 7$, where m is the number of distinct responses, we generate a multi-sensitivity mean pattern by combining responses and reduce sampling errors. Hereafter all pattern-scaled results show the mean of six patterns generated from different combinations of experiments. In previous work, pattern-scaled results have been visualized as either 'sensitivities' to sea-ice loss or to warming, i.e. the partial derivatives in Equation (2), or as 'partial responses' whereby we plot the entire partial derivative terms, including the delta variable. In the case of the latter, this has always been used to decompose the response to general greenhouse warming and as such the deltas are those of that experiment. Here, we seek instead to break down the coupled response to Antarctic sea-ice loss and understand what role tropical warming or Arctic sea-ice loss play.

We demonstrate this idea with Fig. 5, with the coupled model response in "Ant, SOSI+BSI" of zonal-mean temperature in (a) and zonal-mean zonal wind in (b). The partial responses of zonal-mean temperature to SH SIL (c), to tropical warming (e), and to NH SIL (g) reveal that local, surface-amplified Antarctic warming is due mainly to local sea-ice loss but an additional uniform warming from the surface to the tropopause driven by the tropics that extends all the way to the

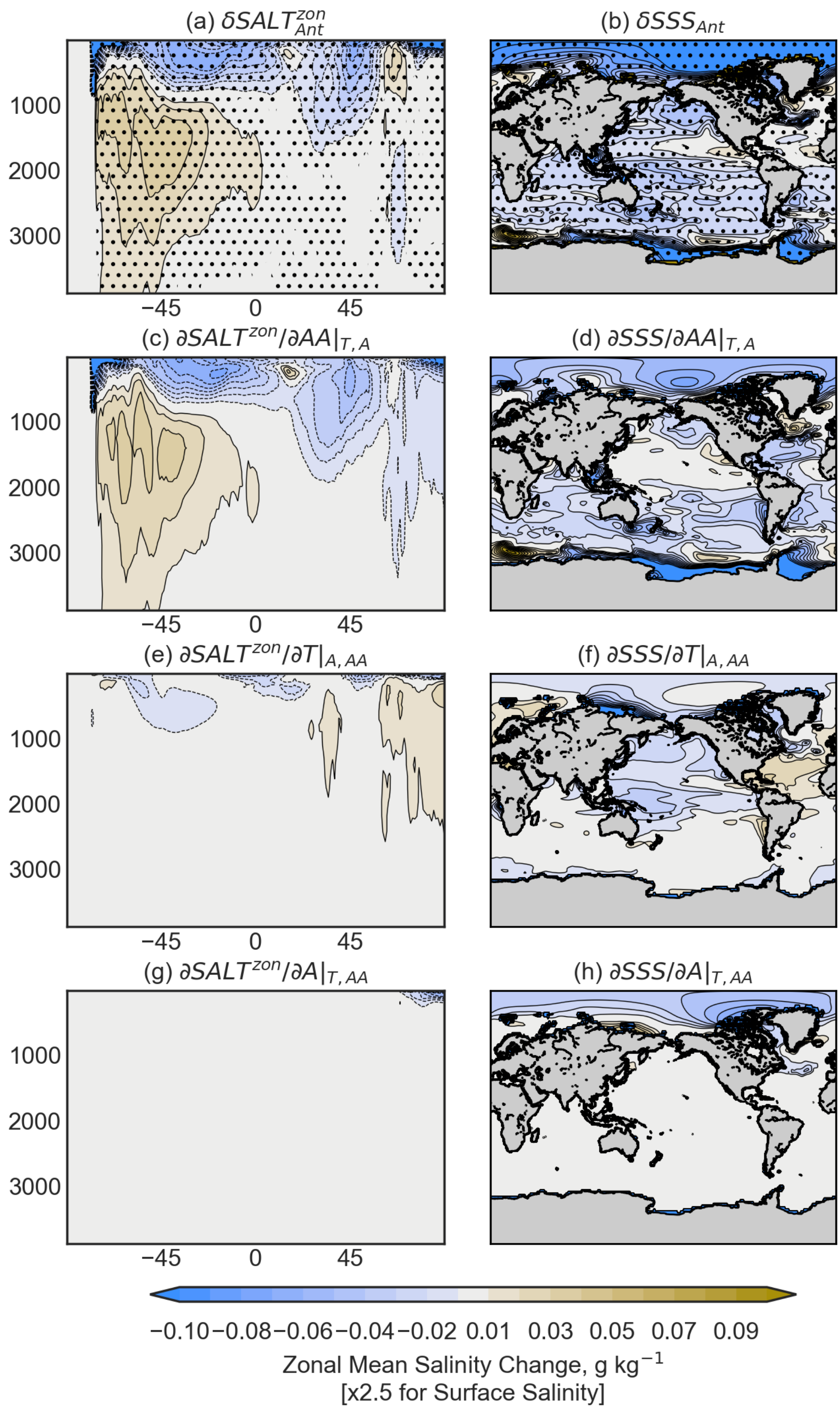

FIG. 7. As in Fig. 5 but for the zonal mean salinity and sea surface salinity responses and partial responses.

other pole. Finally, Arctic sea-ice loss is responsible for a shallow layer of warming at the Arctic surface. The response in zonal-mean zonal wind reveals opposing influences of the tropics and the Antarctic on the Southern Hemisphere eddy-driven jet such that the partial response to Antarctic sea-ice loss is larger than the coupled model response. There is little role for Arctic sea-ice loss in this decomposition.

Given the additivity of ocean variables in our experiments (Fig. 4) we apply pattern-scaling to understand the response of the ocean to Antarctic sea-ice loss. The modelled response of the zonal mean to Antarctic SIL is a broad warming that is carried from pole to pole with maxima in warming under the Antarctic sea-ice, at the edge of the Arctic sea-ice, and in the tropical subsurface (Fig. 6(a)). At the surface, we see a strong warming across the Southern Ocean, in the tropical Pacific and near the sea-ice edge in the Northern Hemisphere (Fig. 6(b)). The pattern-scaling partial responses reveal that subsurface tropical and Antarctic warming can be directly scaled with sea-ice loss (Fig. 6(c)), with a broader warming scaling with tropical warming (Fig. 6(e)). Though not a strong signal in the zonal mean, the pattern-scaling reveals a cooling in the Northern Pacific in the partial response to Antarctic SIL (Fig. 6(d)) that is overwhelmed by even a small amount of tropical warming (Fig. 6(f)). Arctic sea-ice loss generates a small amount of warming near the ice edge ((g),(h)).

Surprisingly, Antarctic sea-ice loss freshens the upper ocean not only in the Southern Hemisphere where the ice is lost (Fig. 7(a)) (except in the seas adjacent to Queen Maud Land (Fig. 7(b))) but throughout the upper ocean all the way to the Arctic. A small salinification region is found co-located with the subtropical warming maxima. At depth in the Southern Hemisphere, we find that Antarctic sea-ice loss causes salinification. The pattern-scaling decomposition reveals that only a small and shallow portion of the Arctic freshening scales with Arctic SIL (Fig. 7(g)), and that the signal scales mainly with Antarctic SIL. More work is needed to understand the mechanism responsible for this surprising result, or whether it is an artifact of the scaling parameters. Finally, tropical warming drives a weak salinification in the Arctic sub-surface, while at the surface, it freshens the Pacific but creates a saltier Atlantic.

d. Scaling with Lapse Rates

Influenced by the results of Feldl et al. (2020), we extend three-parameter pattern-scaling to a new set of more physically-motivated scaling parameters: low-level polar lapse rates and upper tropospheric tropical lapse rates. the Arctic lapse rate feedback is an important contributing component to Arctic Amplification (Pithan and Mauritsen 2014), due to the meridional gradient of the feedback sign, negative at low latitudes and positive at high latitudes. In the tropics, the feedback is negative because the moist adiabatic conditions lead to a larger warming in the upper troposphere than at the surface, creating a larger increase in outgoing longwave radiation per degree of surface warming relative to a vertically uniform warming. On the other hand, the Arctic the lapse rate feedback is positive because stable stratification promotes surface-confined warming. The lapse rate feedback is strongly correlated, across models, with sea-ice loss and increased surface turbulent heat fluxes (Feldl et al. 2020; Boeke et al. 2021), and Cai and Lu (2009) found lapse rate feedback includes the effects of other local feedbacks, such as water vapor, evaporation, moist convection feedbacks. Importantly, Feldl et al. (2020) found distinct mechanisms control the positive high-latitude lower tropospheric lapse rate feedbacks from the negative lapse rate feedbacks of the rest of the atmosphere, which we hope to use to our advantage in decomposing the response to sea-ice loss.

The advantage to using lapse rates as our scaling variables is that it does not use scaling variables, such as sea ice, that we have directly perturbed in the model, but ones that are directly linked to the polar surface and in particular with amplified warming of the polar surface, and can be separated from the rest of the atmosphere.

To compare the results with our original decomposition, Fig. 8 shows the partial responses of zonal-mean temperature and zonal-mean zonal wind to lower tropospheric Antarctic lapse rate changes (a) and (b), to upper tropospheric tropical lapse rate changes (c) and (d), and to lower tropospheric Arctic lapse changes. Qualitatively, each partial response resembles the partial responses in Fig. 5, with some differences in magnitude. These results help show that pattern-scaling results are robust to sensible choices of scaling variables.

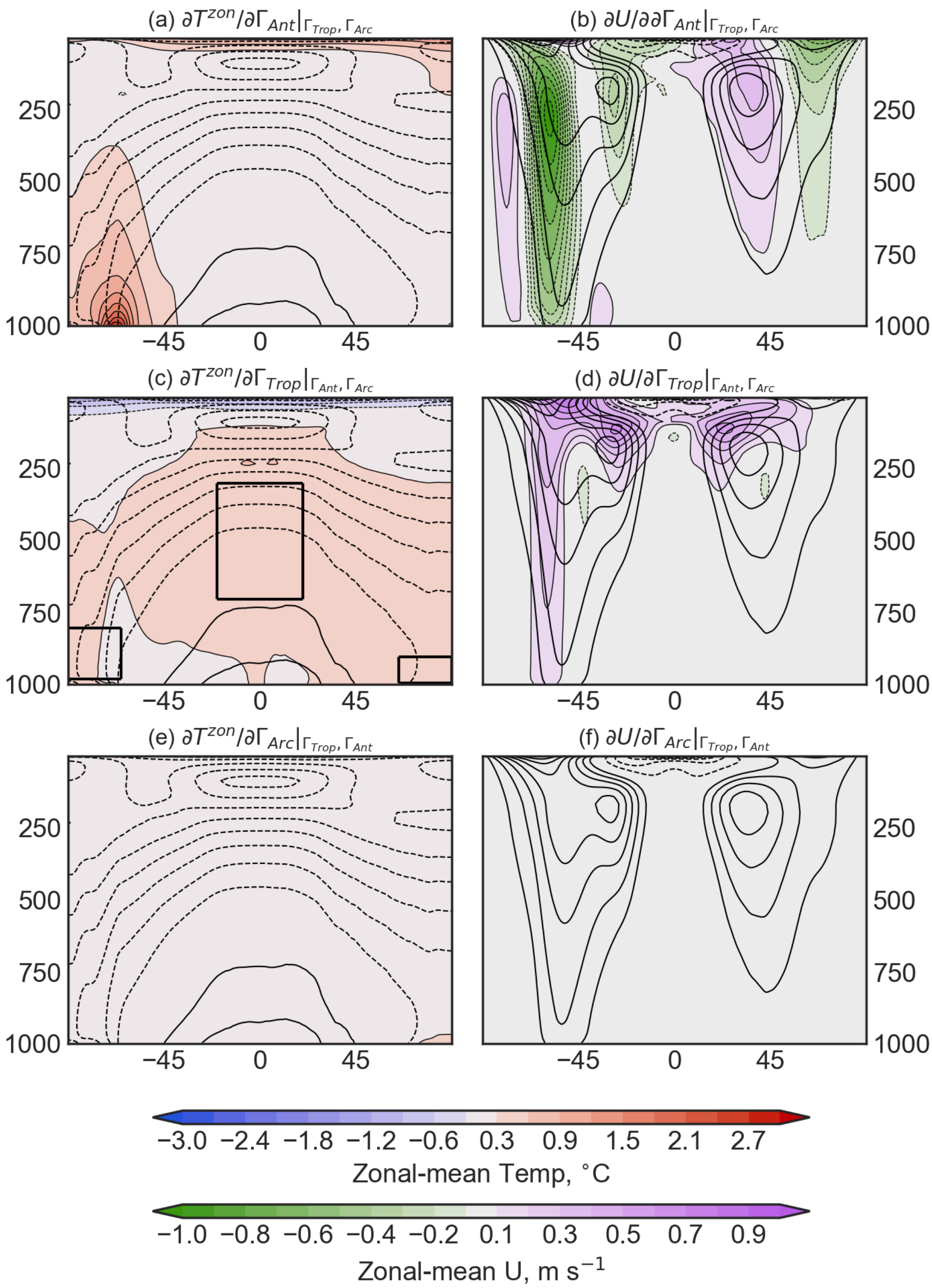

FIG. 8. As in the lower six panels of Fig. 5 but where the decomposition into partial responses use lapse rates as scaling parameters, such that the partial responses in (a) and (b) are to the lower tropospheric Antarctic lapse rate, in (c) and (d) are to the upper tropospheric tropical lapse rate, and in (e) and (f) are to the lower tropospheric Arctic lapse rate. Thick black boxes in (c) indicate the region over which averaging is performed to obtain the scaling parameters.

e. Assessment of regional changes using pattern scaling

Next, we demonstrate how we can use pattern-scaling to reveal and understand specific aspects of the coupled response to Antarctic SIL. The surface temperature response in "Ant" (Fig. 9(a)) is largest along the sea-ice margins of the Southern Hemisphere, over the Antarctic continent, and over the Arctic Ocean. We decompose this area-weighted mean response in two regions: The Arctic (b), and across Siberia (c). The former is chosen because Arctic warming driven by Antarctic sea-ice loss has previously been studied by England et al. (2020b), and the latter is chosen because the sign of the temperature response across Siberia in general greenhouse warming has previously been associated with sea-ice loss (e.g., Mori et al. (2014)).

The modelled response in "Ant" is a broad Arctic warming of 0.80°C, whereas the partial responses reveal that this warming is driven by both the small amounts of tropical warming/increasing tropical upper lapse rate and Arctic sea-ice loss/decreasing lower lapse rate. The partial response to Antarctic sea-ice loss or Antarctic lower lapse rate changes is in fact a very small amount of cooling. Whether the warming is driven more by remote influence or locally depends on the scaling parameter used, and understanding this and how the cooling in response to Antarctic change arises.

Decomposing the weak and broad warming of 0.20°C in "Ant" across Siberia (Figure 9(a),(c)) reveals a tug-of-war between the partial response to tropical and Antarctic change. The tropics act to warm this region while Antarctic sea-ice loss or lapse rate change acts to cool it. The tropical influence overwhelms that of the Antarctic. Again, we find consistency with the decomposition of SSTs in Figure 6(b), where the sea surface cooling extending from Eastern coast of Asia could be arising from the continental cooling.

Another aspect of the response to "Ant" that we note is the deepening of the Aleutian Low in the coupled model (Fig. 10(a)), something previously associated with Arctic sea-ice loss in coupled modelling studies (Hay et al. 2018, 2022). The breakdown into partial responses shown in Fig. 10(b), reveals that the 0.17 hPa decrease in average sea-level pressure over the Aleutian Low region does in fact arise as a response to Antarctic change, and the effects of tropical or Arctic change are small and approximately cancel. It is worth noting here that the various partial responses wont sum exactly to the response in "Ant", as these come from the mean of the six combinations of experiments which each have their own distinct responses. A seemingly curious result here

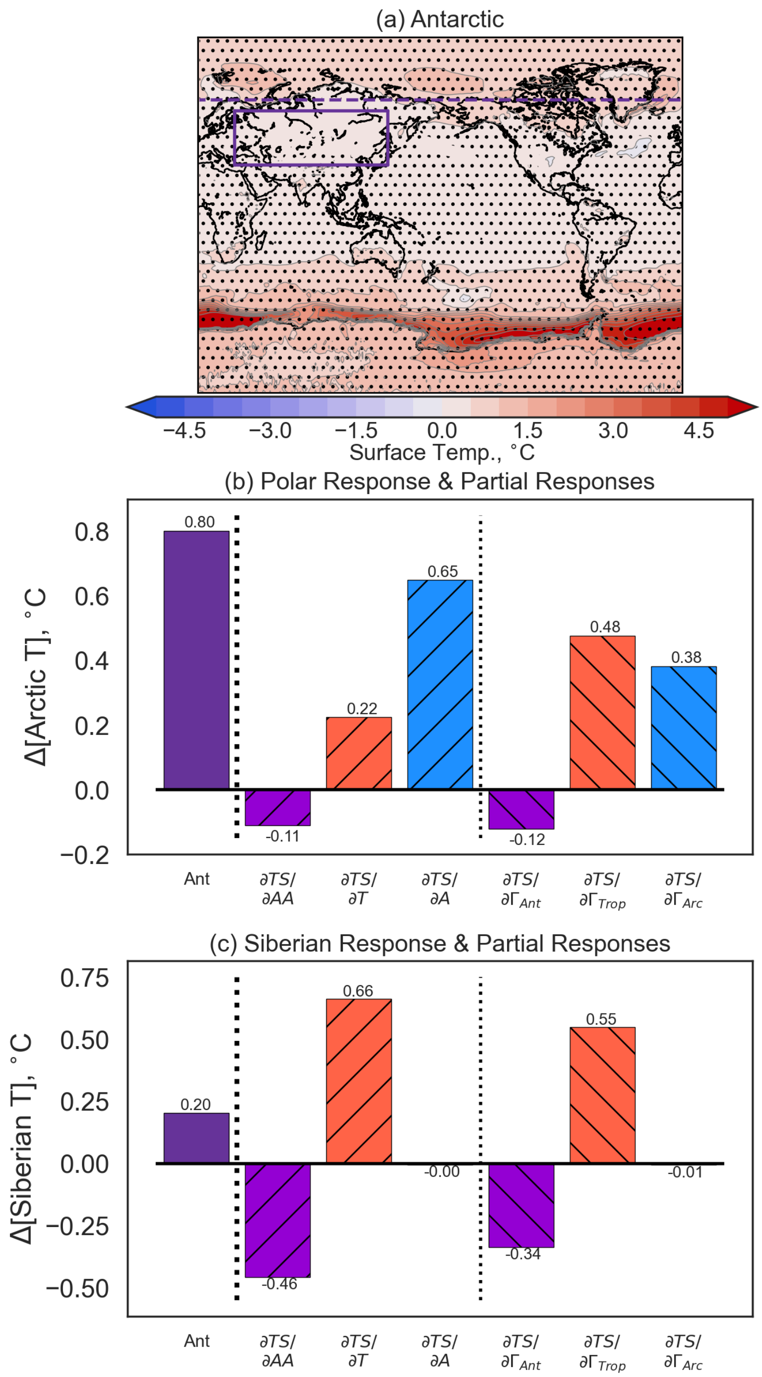

FIG. 9. The surface temperature response to Antarctic sea-ice loss (a), with a dashed purple line to indicate the region we average over to obtain Arctic-mean temperature in (b) and the solid purple box to indicate the region we average over to obtain Siberian temperature in (c). In (b) and (c) are then the area-averaged surface temperature response to Antarctic sea-ice loss broken up in to partial responses as indicated on the x-axes. Stippling in (a) indicates where the surface temperature response to Antarctic sea-ice loss is statistically significant at the 95% confidence level.

whereby Antarctic sea-ice directly drives Northern Hemisphere change, both over Siberia and in the North Pacific is revealed by the pattern-scaling decomposition. Dynamically, there is consistency between Siberian and North Pacific sea-surface cooling and a deepening Aleutian Low, setting up a plausible physical scenario, but a mechanistic explanation and understanding remains to be revealed.

Lastly, the relatively larger role of the Antarctic in the tropics as compared to the Arctic (Fig. 4, right hand column) is examined by decomposing the response of tropical Pacific precipitation in "Ant" (Fig. 11). An equatorward intensification of precipitation is found, particularly evident in the Northern Hemisphere with drying on the northward flank of the Intertropical Convergence Zone (ITCZ). The decomposition into partial responses in the Pacific (Fig. 11(b)) reveals that the southern portion of the moistening is driven by tropical change, whereas the northern portion is driven equally by tropical change and Antarctic change. The drying on the northern flank of the ITCZ mainly driven by Antarctic change, with an additional boost from tropical change. Arctic change plays no role. These results are consistent and robust to the scaling parameters used.

4. Discussion

We have found a relatively larger role for Antarctic sea-ice loss as compared to Arctic sea-ice loss, particularly in the tropics, for the same amount of hemispheric sea-ice loss in the annual mean. However, the Antarctic sea-ice loss experiments generate larger wintertime sea-ice loss than the Arctic ones as a result of the albedo protocol and the geography of each pole: albedo forcing is only effective where there is incoming solar radiation and the sea-ice of the Southern Hemisphere is located at lower latitudes. While this potentially limits a clean comparison of the Arctic and Antarctic cases, we do note that England et al. (2020b) also finds a somewhat larger response to Antarctic sea-ice loss than Arctic sea-ice loss under a different sea-ice loss protocol that does not suffer from the same issue in wintertime.

There is a relatively larger role for Antarctic sea-ice loss in the tropical Pacific, particularly as a component of the full response to greenhouse warming. As we know that climate models have not successfully reproduced trends in Antarctic sea-ice (Roach et al. 2020) or tropical SSTs (Li and Xie 2014), the results we have presented here could potentially suggest that some component of the SST bias as being driven by biased Antarctic sea-ice area.

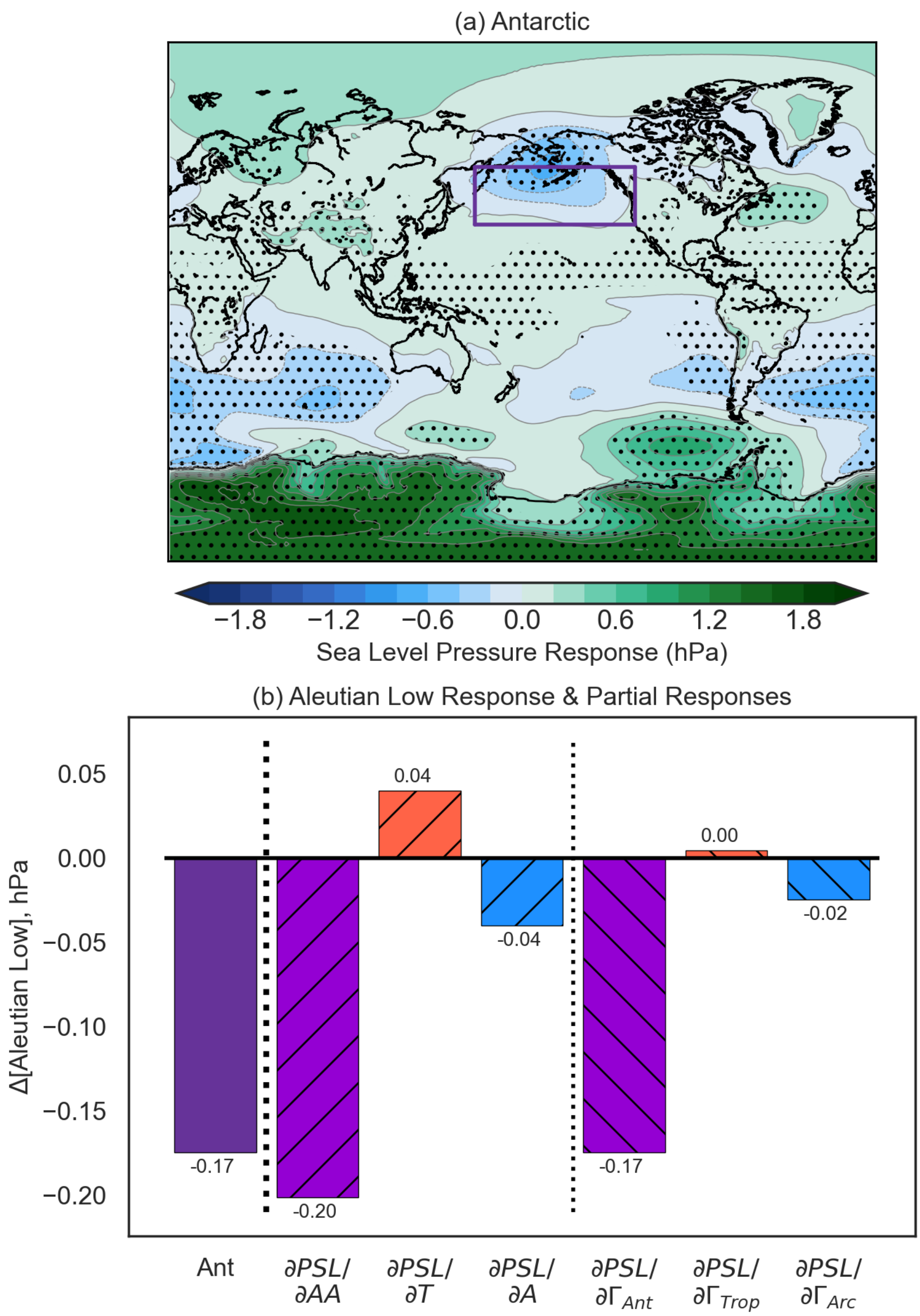

FIG. 10. The sea level pressure response in "Ant, SOSI+BSI" (a), with a solid purple box to indicate the region we average over to obtain area-averaged Aleutian Low pressure for (b). In (b) and is then Aleutian Low response to Antarctic sea-ice loss broken up in to partial responses as indicated on the x-axes. Stippling in (a) indicates where the sea level pressure response to Antarctic sea-ice loss is statistically significant at the 95% confidence level.

However, as with all protocols used in coupled modelling studies to induce sea-ice loss, there is evidence that the warming response to sea-ice loss is likely overestimated (England et al. 2022), as the method itself generates additional heating beyond what is due to sea-ice loss alone. While this is an important factor to keep in mind when analyzing sea-ice loss experiments, it is unlikely to impact our qualitative conclusions. A reduced magnitude of the response directly linked to sea-ice loss is likely.

Two weaknesses of pattern scaling methods are the lack of physical explanation in the results, and the lack of a residual, i.e. it assumes a climate response can be fully explained by the chosen scaling factors. To attempt to account for the latter, we have used multiple experiment combinations in generating the partial responses to minimize spurious results and hopefully determine the most accurate partial responses. For the former, we attempt to take the whole picture of partial responses to try to build a physically consistent story that may then be tested using different approaches. For example, we find that there is a direct response to Antarctic change throughout the ocean that extends into the Northern Hemisphere and is consistent between the surface, sea-surface subsurface temperature partial responses, between the Aleutian Low, precipitation, and salinity partial responses. While we can postulate that the ocean is driving the atmosphere due to a lack of response in the Northern Hemisphere in similar atmosphere-only experiments (England et al. 2018; Ayres et al. 2022), the coupling is two-way and complex and could potentially only be understood by examining, for example, the transient evolution of the response to Antarctic sea-ice loss.

5. Conclusions

Using a set coupled model sea ice and snow albedo perturbation experiments alongside a CO_2 doubling experiment, we find a globally relevant role for Antarctic sea-ice loss in CESM1. In both the atmosphere and the ocean, the zonal mean temperature response to sea-ice loss from either hemisphere replicates that of greenhouse warming by CO_2, something that has been termed the "mini global warming" for the atmospheric response Deser et al. (2015). We show here, in agreement with Ayres et al. (2022), that the the ocean's response also exhibits this global character. Using an spatial correlation analysis we find a larger correspondence between the response to sea-ice loss in both hemispheres concurrently and that from the Antarctic alone, particularly in the tropical Pacific, quantifying the larger role of Antarctic change.

For the first time, we expand the two-parameter pattern scaling of Blackport and Kushner (2017) to include a third parameter related to Antarctic change. We also explore the use of other scaling parameters that are perhaps more physically relevant and find that the decomposition of the response into partial responses is qualitatively robust, allowing us to re-frame and generalize the response into parts that scale with, or partial responses to, Antarctic change, tropical change, and Arctic change.

Applying this improved version of multi-parameter pattern-scaling to the coupled model response to Antarctic sea-ice loss, we demonstrate how this can be used to disentangle the distinct role of Antarctic change from that which arises from tropical or Arctic change that is itself driven by Antarctic sea-ice loss. The method reveals details of the response and creates a plausible physical basis that can then be tested via targeted modelling experiments.

Given this, we have found that the partial response to Antarctic change can play an important role not just locally but in the tropics and into the Northern Hemisphere. This includes a subsurface warming and salinification of the ocean just north of the Equator, as well as an equatorward shift of the precipitation in this same region. Further North, a cooling of Siberia and the North Pacific sea surface, where there is also a freshening that extends to depth and in to the Arctic, alongside a deepening of the Aleutian Low. Some of these aspects were evident from the coupled modelling results (e.g. the Aleutian Low, freshening North Pacific, equatorward intensification of the precipitation), while others were only revealed by the decomposition (e.g. Siberian, Arctic, and North Pacific cooling). Additionally, these results show that even small amounts of tropical change as those found in “Ant”, can easily overwhelm the impact of Antarctic change, of particular relevance for understanding the role of the Antarctic in the response to greenhouse warming.

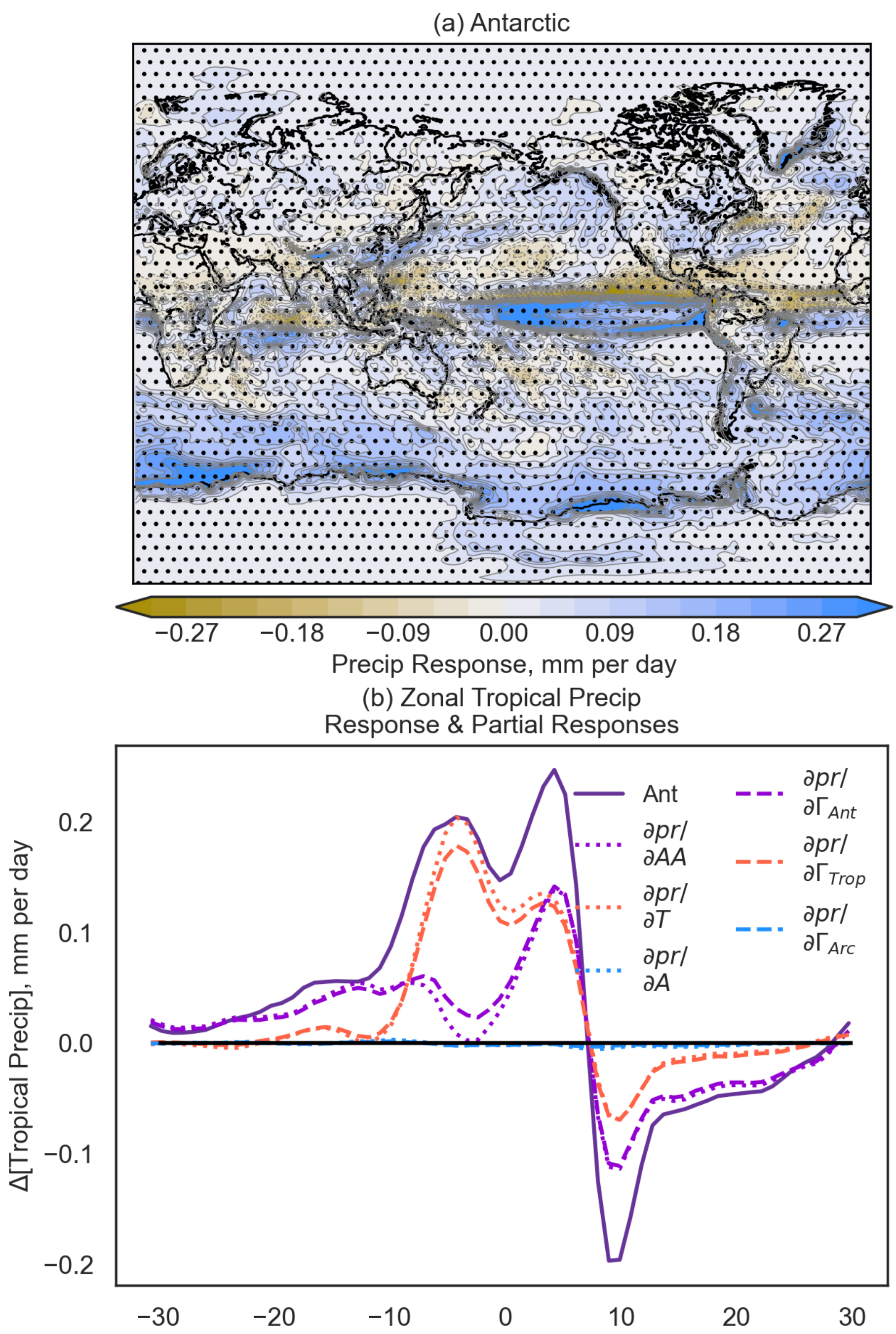

FIG. 11. The precipitation response in "Ant, SOSI+BSI" (a) and the zonal response of precipitation from -30°N to 30°N over the Pacific Ocean broken up in to its component partial responses as indicated by the legend. Stippling in (a) indicates where the precipitation response to Antarctic sea-ice loss is statistically significant at the 95% confidence level.

Acknowledgments. This work was supported by a grant from the U.S. Department of Energy Grant DE-SC0019407.

Data availability statement. Output from the simulations used in this study is stored with the Digital Research Alliance of Canada and subsets of it can be obtained by contacting the authors.

APPENDIX

Three-parameter pattern scaling

Classically, pattern scaling posits that spatial patterns of the externally forced response of some variable, Z, are robust throughout the transient evolution when scaled by the change in global mean temperature change, δT:

$$\delta Z(t, x, y, s) = z(x, y, s)\delta T(t). \tag{A1}$$

Here x, y are the spatial coordinates, t is the time coordinate, and s specifies the averaging period (e.g., monthly or seasonal mean). $z(x, y, s)$ then represents the time-invariant pattern of the response of Z.

In this case, we will require $m \geq 3$, where m is the index of a particular simulation, to obtain the system of equations required to solve for the three sensitivity patterns, and we can write Equation 2 succinctly in matrix notation as:

$$\begin{pmatrix} \delta Z_1 \\ \delta Z_2 \\ \delta Z_3 \end{pmatrix} = \begin{pmatrix} \delta A_1 & \delta AA_1 & \delta T_1 \\ \delta A_2 & \delta AA_2 & \delta T_2 \\ \delta A_3 & \delta AA_3 & \delta T_3 \end{pmatrix} \begin{pmatrix} \frac{\partial Z}{\partial A}\big|_{T,AA} \\ \frac{\partial Z}{\partial AA}\big|_{T,A} \\ \frac{\partial Z}{\partial T}\big|_{A,AA} \end{pmatrix} \tag{A2}$$

Assuming that the above matrix is invertible, we invert to solve for the sensitivities. This inversion yields,

$$\begin{pmatrix} \frac{\partial Z}{\partial A}\big|_{T,AA} \\ \frac{\partial Z}{\partial AA}\big|_{T,A} \\ \frac{\partial Z}{\partial T}\big|_{A,AA} \end{pmatrix} = \frac{1}{\alpha} \begin{pmatrix} \beta & \gamma & \epsilon \\ \zeta & \eta & \iota \\ \kappa & \lambda & \mu \end{pmatrix} \begin{pmatrix} \delta Z_1 \\ \delta Z_2 \\ \delta Z_3 \end{pmatrix} \tag{A3}$$

such that,

$$\left.\frac{\partial Z}{\partial A}\right|_{T,AA} = \frac{1}{\alpha}[\beta\delta Z_1 + \gamma\delta Z_2 + \epsilon\delta Z_3] \tag{A4}$$

$$\left.\frac{\partial Z}{\partial AA}\right|_{T,A} = \frac{1}{\alpha}[\zeta\delta Z_1 + \eta\delta Z_2 + \iota\delta Z_3] \tag{A5}$$

$$\left.\frac{\partial Z}{\partial AA}\right|_{A,AA} = \frac{1}{\alpha}[\kappa\delta Z_1 + \lambda\delta Z_2 + \mu\delta Z_3] \tag{A6}$$

where

$$\alpha = \delta A_1\beta + \delta AA_1\zeta + \delta T_1\kappa \tag{A7}$$

$$\beta = \delta AA_2\delta T_3 - \delta AA_3\delta T_2 \tag{A8}$$

$$\gamma = \delta AA_3\delta T_1 - \delta AA_1\delta T_3 \tag{A9}$$

$$\epsilon = \delta AA_1\delta T_2 - \delta AA_2\delta T_1 \tag{A10}$$

$$\zeta = \delta A_3\delta T_2 - \delta A_2\delta T_3 \tag{A11}$$

$$\eta = \delta A_1\delta T_3 - \delta A_3\delta T_1 \tag{A12}$$

$$\iota = \delta A_2\delta T_1 - \delta A_1\delta T_2 \tag{A13}$$

$$\kappa = \delta A_2\delta AA_3 - \delta A_3\delta AA_2 \tag{A14}$$

$$\lambda = \delta A_3\delta AA_1 - \delta A_1\delta AA_3 \tag{A15}$$

$$\mu = \delta A_1\delta AA_2 - \delta A_2\delta AA_1 \tag{A16}$$

References

Ayres, H., and J. Screen, 2019: Multimodel analysis of the atmospheric response to Antarctic sea ice loss at quadrupled CO2. *Geophysical Research Letters*, 2019GL083653, https://doi.org/10.1029/2019GL083653.

Ayres, H. C., J. A. Screen, E. W. Blockley, and T. J. Bracegirdle, 2022: The coupled atmosphere–ocean response to Antarctic sea ice loss. *Journal of Climate*, **35**, 4665–4685, https://doi.org/10.1175/JCLI-D-21-0918.1.

Bader, J., M. Flügge, N. G. Kvamstø, M. D. Mesquita, and A. Voigt, 2013: Atmospheric winter response to a projected future Antarctic sea-ice reduction: A dynamical analysis. *Climate Dynamics*, **40**, 2707–2718, https://doi.org/10.1007/s00382-012-1507-9.

Blackport, R., and P. J. Kushner, 2016: The transient and equilibrium climate response to rapid summertime sea ice loss in CCSM4. *Journal of Climate*, **29**, 401–417, https://doi.org/10.1175/JCLI-D-15-0284.1.

Blackport, R., and P. J. Kushner, 2017: Isolating the atmospheric circulation response to Arctic sea ice loss in the coupled climate system. *Journal of Climate*, **30**, 2163–2185, https://doi.org/10.1175/JCLI-D-16-0257.1.

Boeke, R. C., P. C. Taylor, and S. A. Sejas, 2021: On the nature of the Arctic's positive lapse-rate feedback. *Geophysical Research Letters*, **48**, e2020GL091 109, https://doi.org/10.1029/2020GL091109.

Briegleb, P., and B. Light, 2007: A delta-eddington mutiple scattering parameterization for solar radiation in the sea ice component of the community climate system model. 1-100 pp., https://doi.org/10.5065/D6B27S71.

Bronselaer, B., M. Winton, S. M. Griffies, W. J. Hurlin, K. B. Rodgers, O. V. Sergienko, R. J. Stouffer, and J. L. Russell, 2018: Change in future climate due to Antarctic meltwater. *Nature*, **564**, 53–58, https://doi.org/10.1038/s41586-018-0712-z.

Cai, M., and J. Lu, 2009: A new framework for isolating individual feedback processes in coupled general circulation climate models. part ii: Method demonstrations and comparisons. *Climate Dynamics*, **32**, 887–900, https://doi.org/https://doi.org/10.1007/s00382-008-0424-4.

Deser, C., L. Sun, R. A. Tomas, and J. Screen, 2016: Does ocean coupling matter for the northern extratropical response to projected Arctic sea ice loss? *Geophysical Research Letters*, **43**, 2149–2157, https://doi.org/10.1002/2016GL067792.

Deser, C., R. A. Tomas, and L. Sun, 2015: The role of ocean–atmosphere coupling in the zonal-mean atmospheric response to Arctic sea ice loss. *Journal of Climate*, **28**, 2168–2186, https://doi.org/10.1175/JCLI-D-14-00325.1.

England, M., L. Polvani, and L. Sun, 2018: Contrasting the Antarctic and Arctic atmospheric responses to projected sea ice loss in the late twenty-first century. *Journal of Climate*, **31**, 6353–6370, https://doi.org/10.1175/JCLI-D-17-0666.1.

England, M. R., I. Eisenman, and T. J. W. Wagner, 2022: Spurious climate impacts in coupled sea ice loss simulations. *Journal of Climate*, **35**, 1–38, https://doi.org/10.1175/JCLI-D-21-0647.1.

England, M. R., L. M. Polvani, and L. Sun, 2020a: Robust Arctic warming caused by projected Antarctic sea ice loss robust Arctic warming caused by projected Antarctic sea ice loss. *Environ. Res. Lett*, **15**, 104 005, https://doi.org/10.1088/1748-9326/abaada.

England, M. R., L. M. Polvani, L. Sun, and C. Deser, 2020b: Tropical climate responses to projected Arctic and Antarctic sea-ice loss. *Nature Geoscience*, https://doi.org/10.1038/s41561-020-0546-9.

Eyring, V., S. Bony, G. A. Meehl, C. A. Senior, B. Stevens, R. J. Stouffer, and K. E. Taylor, 2016: Overview of the coupled model intercomparison project phase 6 (CMIP6) experimental design and organization. *Geoscientific Model Development*, **9**, 1937–1958, https://doi.org/10.5194/gmd-9-1937-2016.

Feldl, N., S. Po-Chedley, H. K. A. Singh, S. Hay, and P. J. Kushner, 2020: Sea ice and atmospheric circulation shape the high-latitude lapse rate feedback. *npj Climate and Atmospheric Science*, **3**, 41, https://doi.org/10.1038/s41612-020-00146-7.

Gagné, M.-E., N. P. Gillett, and J. C. Fyfe, 2015: Observed and simulated changes in Antarctic sea ice extent over the past 50 years. *Geophysical Research Letters*, **42**, 90–95, https://doi.org/10.1002/2014GL062231.

Hay, S., P. J. Kushner, R. Blackport, and K. E. McCusker, 2018: On the relative robustness of the climate response to high-latitude and low-latitude warming. *Geophysical Research Letters*, **45**, https://doi.org/10.1029/2018GL077294.

Hay, S., and Coauthors, 2022: Separating the influences of low-latitude warming and sea ice loss on northern hemisphere climate change. *Journal of Climate*, **35**, 2327–2349, https://doi.org/10.1175/JCLI-D-21-0180.1.

Kang, S. M., I. M. Held, D. M. Frierson, and M. Zhao, 2008: The response of the ITCZ to extratropical thermal forcing: Idealized slab-ocean experiments with a gcm. *Journal of Climate*, **21**, 3521–3532, https://doi.org/10.1175/2007JCLI2146.1.

Kang, S. M., L. M. Polvani, J. C. Fyfe, and M. Sigmond, 2011: Impact of polar ozone depletion on subtropical precipitation. *Science*, **332**, 951–954, https://doi.org/10.1126/science.l202584.

Kay, J. E., and Coauthors, 2015: The community earth system model (CESM) large ensemble project: A community resource for studying climate change in the presence of internal climate variability. *Bulletin of the American Meteorological Society*, **96**, 1333–1349, https://doi.org/10.1175/BAMS-D-13-00255.1.

Kidston, J., A. S. Taschetto, D. W. J. Thompson, and M. H. England, 2011: The influence of southern hemisphere sea-ice extent on the latitude of the mid-latitude jet stream. *Geophysical Research Letters*, **38**, https://doi.org/10.1029/2011GL048056.

Li, G., and S. P. Xie, 2014: Tropical biases in CMIP5 multimodel ensemble: The excessive equatorial pacific cold tongue and double itcz problems. *Journal of Climate*, **27**, 1765–1780, https://doi.org/10.1175/JCLI-D-13-00337.1.

Marvel, K., G. A. Schmidt, D. Shindell, C. Bonfils, A. N. Legrande, L. Nazarenko, and K. Tsigaridis, 2015: Do responses to different anthropogenic forcings add linearly in climate models? *Environmental Research Letters*, **10**, 104 010, https://doi.org/10.1088/1748-9326/10/10/104010.

Massom, R. A., and Coauthors, 2001: Snow on Antarctic sea ice. *Reviews of Geophysics*, **39**, 413–445, https://doi.org/10.1029/2000RG000085.

McCusker, K. E., P. J. Kushner, J. C. Fyfe, M. Sigmond, V. V. Kharin, and C. M. Bitz, 2017: Remarkable separability of circulation response to Arctic sea ice loss and greenhouse gas forcing. *Geophysical Research Letters*, **44**, 7955–7964, https://doi.org/10.1002/2017GL074327.

Mori, M., M. Watanabe, H. Shiogama, J. Inoue, and M. Kimoto, 2014: Robust Arctic sea-ice influence on the frequent eurasian cold winters in past decades. *Nature Geoscience*, **7**, 869–873, https://doi.org/10.1038/ngeo2277.

Oudar, T., E. Sanchez-Gomez, F. Chauvin, J. Cattiaux, L. Terray, and C. Cassou, 2017: Respective roles of direct ghg radiative forcing and induced Arctic sea ice loss on the northern hemisphere atmospheric circulation. *Climate Dynamics*, **49**, 3693–3713, https://doi.org/10.1007/s00382-017-3541-0.

Perovich, D. K., T. C. Grenfell, B. Light, and P. V. Hobbs, 2002: Seasonal evolution of the albedo of multiyear actic sea ice. *Journal of Geophysical Research C: Oceans*, **107**, SHE 20–1, https://doi.org/10.1029/2000jc000438.

Pithan, F., and T. Mauritsen, 2014: Arctic amplification dominated by temperature feedbacks in contemporary climate models. *Nature Geoscience*, **7**, 181–184, https://doi.org/10.1038/ngeo2071.

Roach, L. A., and Coauthors, 2020: Antarctic sea ice area in CMIP6. *Geophysical Research Letters*, **47**, https://doi.org/10.1029/2019GL086729.

Screen, J. A., and R. Blackport, 2019: How robust is the atmospheric response to projected Arctic sea ice loss across climate models? *Geophysical Research Letters*, **46**, 11 406–11 415, https://doi.org/10.1029/2019GL084936.

Screen, J. A., and Coauthors, 2018: Consistency and discrepancy in the atmospheric response to Arctic sea-ice loss across climate models. *Nature Geoscience*, **11**, 155–163, https://doi.org/10.1038/s41561-018-0059-y.

Shiogama, H., D. A. Stone, T. Nagashima, T. Nozawa, and S. Emori, 2013: On the linear additivity of climate forcing-response relationships at global and continental scales. *International Journal of Climatology*, **33**, 2542–2550, https://doi.org/10.1002/joc.3607.

Singh, H. A., L. M. Polvani, and P. J. Rasch, 2019: Antarctic sea ice expansion, driven by internal variability, in the presence of increasing atmospheric CO2. *Geophysical Research Letters*, 2019GL083758, https://doi.org/10.1029/2019GL083758.

Smith, D. M., N. J. Dunstone, A. A. Scaife, E. K. Fiedler, D. Copsey, and S. C. Hardiman, 2017: Atmospheric response to Arctic and Antarctic sea ice: The importance of ocean-atmosphere coupling and the background state. *Journal of Climate*, **30**, 4547–4546, https://doi.org/10.1175/JCLI-D-16-0564.1.

Stott, P. A., N. P. Gillett, G. C. Hegerl, D. J. Karoly, D. A. Stone, X. Zhang, and F. Zwiers, 2010: Detection and attribution of climate change: a regional perspective. *Wiley Interdisciplinary Reviews: Climate Change*, **1**, 192–211, https://doi.org/10.1002/wcc.34.

Sun, L., M. Alexander, and C. Deser, 2018: Evolution of the global coupled climate response to Arctic sea ice loss during 1990–2090 and its contribution to climate change. *Journal of Climate*, **31**, 7823–7843, https://doi.org/10.1175/JCLI-D-18-0134.1.

Sun, L., C. Deser, R. A. Tomas, and M. Alexander, 2020: Global coupled climate response to polar sea ice loss: Evaluating the effectiveness of different ice-constraining approaches. *Geophysical Research Letters*, **47**, https://doi.org/10.1029/2019GL085788.

Swart, N. C., and J. C. Fyfe, 2013: The influence of recent Antarctic ice sheet retreat on simulated sea ice area trends. *Geophysical Research Letters*, **40**, 4328–4332, https://doi.org/10.1002/grl.50820.

Talley, L. D., 2013: Closure of the global overturning circulation through the indian, pacific, and southern oceans: Schematics and transports. *Oceanography*, **26**, 80–97, https://doi.org/10.5670/oceanog.2013.07.

Tomas, R. A., C. Deser, L. Sun, R. A. Tomas, , and C. Deser, 2016: The role of ocean heat transport in the global climate response to projected Arctic sea ice loss. *Journal of Climate*, **29**, 6841–6859, https://doi.org/10.1175/JCLI-D-15-0651.1.

Turner, J., T. J. Bracegirdle, T. Phillips, G. J. Marshall, and J. S. Hosking, 2013: An initial assessment of Antarctic sea ice extent in the CMIP5 models. *Journal of Climate*, **26**, 1473–1484, https://doi.org/10.1175/JCLI-D-12-00068.1.

Zappa, G., F. Pithan, and T. G. Shepherd, 2018: Multimodel evidence for an atmospheric circulation response to Arctic sea ice loss in the CMIP5 future projections. *Geophysical Research Letters*, **45**, 1011–1019, https://doi.org/10.1002/2017GL076096.

Zunz, V., H. Goosse, and F. Massonnet, 2013: How does internal variability influence the ability of CMIP5 models to reproduce the recent trend in southern ocean sea ice extent? *Cryosphere*, **7**, 451–468, https://doi.org/10.5194/tc-7-451-2013.